Field-free anomalous junction and superconducting diode effect in spin-split superconductor/topological insulator junctions

T. H. Kokkeler,[1,2,*] A. A. Golubov,[2] and F. S. Bergeret[3,1]

[1]*Donostia International Physics Center (DIPC), 20018 Donostia–San Sebastián, Spain*

[2]*Interfaces and Correlated Electron Systems, Faculty of Science and Technology, University of Twente, P.O. Box 217, 7500 AE Enschede, The Netherlands*

[3]*Centro de Física de Materiales (CFM-MPC) Centro Mixto CSIC-UPV/EHU, E-20018 Donostia-San Sebastián, Spain*

(Received 4 October 2022; accepted 28 November 2022; published 7 December 2022; corrected 23 December 2022)

We study the transport properties of a diffusive Josephson junction between two spin-split superconductors (SCs) made of SC-ferromagnetic insulator bilayers on top of a three-dimensional topological insulator. We derive the corresponding Usadel equation describing the quasiclassical Green's functions in these systems and first solve the equation analytically in the weak-proximity case. We demonstrate the appearance of an anomalous phase in the absence of an external magnetic field. We also explore nonreciprocal electronic transport. Specifically, we calculate the diode efficiency of the junction η by solving the Usadel equation. We obtain a sizable diode effect even at zero applied magnetic field. We discuss how the diode efficiency η depends on the different parameters and find a nonmonotonic behavior of η with temperature.

DOI: 10.1103/PhysRevB.106.214504

I. INTRODUCTION

Recent advances attracting attention in superconductivity research are effects related to the nonreciprocal charge transport [1,2], particularly the superconducting (SC) diode effect [3–13]. A mesoscopic junction with SCs is called a SC diode if the critical current is different for opposite current directions. That is, for a SC diode, the minimum $I_- = \min_\phi I_s(\phi)$ and maximum $I_+ = \max_\phi I_s(\phi)$ of the current phase relation (CPR) are unequal in magnitude. If a current I flows in such a junction, with $\min(|I_-|, I_+) < I < \max(|I_-|, I_+)$, in one direction, it is a supercurrent, whereas in the other direction, it is a dissipative current. In a conventional Josephson junction, the critical current is the same in both directions; the CPR has the following symmetry: $I(-\phi) = -I(\phi)$ [14]. This relation holds if either time-reversal symmetry or inversion symmetry is present in the system [15,16].

The SC diode effect can thus only be obtained if both time-reversal symmetry and inversion symmetry are broken [5,6]. Time-reversal symmetry can be broken by a magnetic field. On the other hand, inversion symmetry can be broken intrinsically, such as in topological insulators (TIs) [17–19] or SCs with Rashba spin-orbit coupling [20–27]. Inversion symmetry can also be broken by asymmetry of the junction geometry [28] or asymmetry of the device originated in fabrication [10].

If both time-reversal symmetry and inversion symmetry are broken, in general, $I(-\phi) \neq -I(\phi)$, and thus, possibly $I(\phi = 0) \neq 0$. Such junctions, for which the current vanishes at a nonzero phase difference, are called ϕ_0 junctions [21]. In weak coupling Josephson junctions, the CPR is proportional to $\sin(\phi + \phi_0)$; hence, in this regime, one cannot observe the diode effect. However, if higher harmonics contribute to the current, in general, $I_+ \neq |I_-|$, and the diode effect can be observed [7,9,11,12].

One way of breaking time-reversal symmetry without an external magnetic field is to attach a ferromagnetic insulator (FI) to the SC (FIS). FIS systems have been discussed extensively in the literature [29–32]. The exchange interaction between the localized magnetic moments of the FI and the itinerant electrons in the SC leads to a spin split in the density of states of the latter. Spin-split SCs form an active field of research with varying directions [33–39].

In this paper, we investigate the diode effect in a Josephson junction consisting of spin-split SC electrodes on the two-dimensional (2D) surface of a disordered three-dimensional (3D) TI. Specifically, our setup consists of two spin-split SCs (FIS) placed on top of a TI, see Fig. 1(a). Time-reversal symmetry is broken by the spin-splitting in the SC, whereas inversion symmetry is broken because we consider only the top surface of the TI. Thus, the conditions to have a ϕ_0 effect are fulfilled even without an external magnetic field. Using the linearized Usadel equation, we first show analytically that the CPR in such a junction exhibits the ϕ_0 effect. Going beyond the linear regime, we compute the diode efficiency. Even in the case of low-transmission FIS/TI interfaces, we obtain an efficiency of 1%. By increasing the interface transmission, the efficiency can reach values >7%. We also find that, for short junctions, the efficiency is maximized at a finite temperature independent of the strength of the exchange field.

This paper is structured as follows. In Sec. II, we introduce the setup and the basic equations. We derive the Usadel equation for a diffusive TI in proximity with a spin-split SC. In Sec. III, we focus on analytical results that can be obtained by linearizing the Usadel equation, which is valid under the

*tim.kokkeler@dipc.org

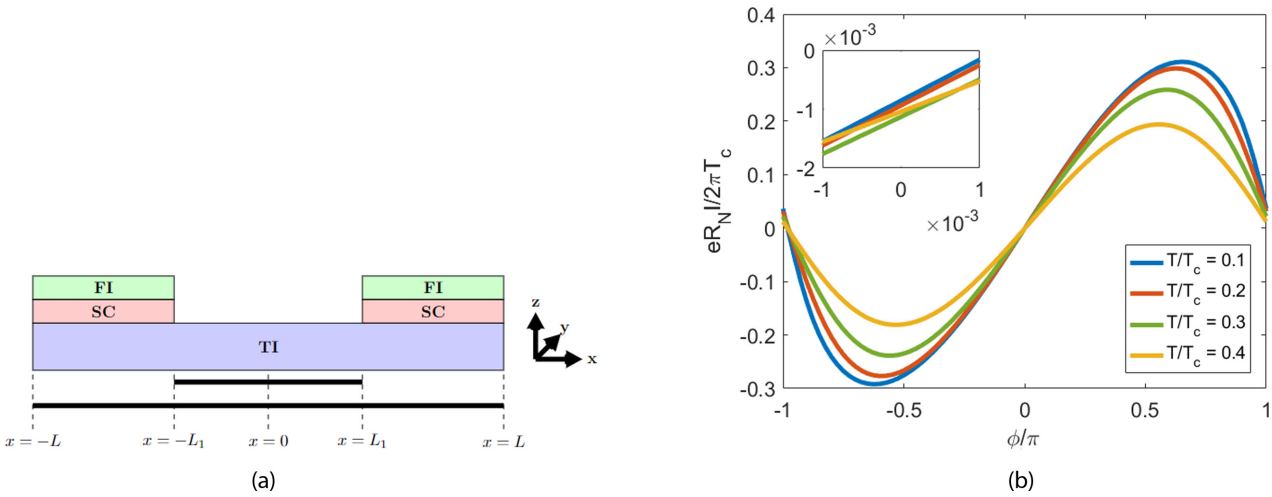

FIG. 1. (a) Sketch of the junction under consideration. (b) The current phase relation (CPR) of the ferromagnetic insulator/superconductor (FIS)-topological insulator (TI)-FIS junction for different temperatures. The parameters chosen are $\frac{\gamma_0}{E_{\rm Th}} = \frac{\Delta_0}{E_{\rm Th}} = \frac{5h}{2E_{\rm Th}} = 25$, $\frac{L_1}{L} = \frac{1}{10}$, and $\frac{l}{L} = 0.08 \ll 1$. Inset: Zoom-in of the CPR around $\phi = 0$.

assumption that the proximity effect is small. Even though, in this limit, the CPR contains only the first harmonic and thus has no diode effect, we can determine the condition for observation of the anomalous Josephson currents. The latter is the precursor of a diode effect in the nonlinearized equation. We also show that the ϕ_0 effect is suppressed by impurity scattering. In Sec. IV, we go beyond the linear regime and present our numerical results for the nonlinear equation and the diode efficiency as a function of the temperature for different values of the exchange field, length of the junction, and transparency of the interfaces. Finally, in Sect. V, we conclude and propose real material combinations to test our predictions. Throughout the paper, it is assumed that $\hbar = k_{\rm B} = 1$.

II. THE SYSTEM AND BASIC EQUATIONS

We consider the FIS-TI-FIS system shown in Fig. 1(a). An FIS can be realized by placing a FI on top of a SC film with a conventional s-wave pair potential. The thickness of the latter is assumed to be small compared with its coherence length, so that we can assume a homogeneous splitting field in the SC induced by the magnetic proximity effect [40]. In this setup, a current can flow through the top surface of the TI from one FIS to the other. Because the system is finite in the x direction, no current can flow at $x = \pm L/2$, where L is the length of the TI. We denote by L_1 the length of the TI between the two FIS electrodes.

We assume that the transport at the TI surface is diffusive and can be described by the Usadel equation: the derivation of this equation for our system closely resembles the derivation of the Usadel equation for a TI in an exchange field as presented in Refs. [41,42]. However, whereas superconductivity in the systems discussed in these papers is introduced as an effective pair potential, for the spin-split SC, a different approach is taken.

We incorporate the effect of the spin-split SC as a self-energy term $\bar{\Sigma}_s$. For the self-energy, we follow the approach in Ref. [43], in which the self-energy due to tunneling between the TI and the SC is introduced. Up to second order in the tunneling parameter T_1 between the TI and the SC, it is given by

$$\bar{\Sigma}_s = T_1^2 \rho_S \check{\tau}_3 \sigma_0 \bar{G}'_S \sigma_0 \check{\tau}_3 = T_1^2 \rho_S \bar{G}_S = \gamma_0 \bar{G}_S, \tag{1}$$

where $\gamma_0 = T_1^2 \rho_S$ is the tunneling energy scale and ρ_S the effective 2D density of states of the SC at the interface [43]. The parameter γ_0 is restricted because our assumption that only terms of second order in T_1 need to be considered implies $T_1^2 \rho_{\rm TI} \ll \Delta_0$, where $\rho_{\rm TI}$ is the density of states of the surface of the TI. This implies that $\gamma_0 \ll \Delta_0 \frac{\rho_S}{\rho_{\rm TI}}$. Here, σ_0 is the identity matrix in spin space, and $\check{\tau}_3$ is the third Pauli matrix in electron-hole space. Here, $\bar{G}'_S$ is the momentum-integrated Green's function (GF) in the spin-split SC and $\bar{G}_S = \check{\tau}_3 \sigma_0 \bar{G}'_S \sigma_0 \check{\tau}_3$ is introduced to shorten notation. Note that the only effect of this transformation by $\check{\tau}_3 \sigma_0$ is to negate the pair amplitudes. We go up to second order in tunneling and neglect the inverse proximity effect of the TI on the SC. The self-energy term appears as an added term in the commutator on the left-hand side of the Eilenberger equation. The Eilenberger equation thus reads, using the same presentation in spin-Nambu space as in Ref. [41],

$$\frac{v_{\rm F}}{2}\{[\eta_j, \nabla_j \check{g}(1 + \vec{n}_{\rm F} \cdot \vec{\eta})]\} = \Big[\check{g}(1 + \vec{n}_{\rm F} \cdot \eta), \omega_n \check{\tau}_3 + \Gamma(x) \bar{G}_S + \frac{\langle \check{g}(1 + \vec{n}_{\rm F} \cdot \vec{\eta})\rangle}{2\tau}\Big], \tag{2}$$

where $\{\cdot, \cdot\}$ denotes the anticommutator and $[\cdot, \cdot]$ the commutator. In our notation, $\check{g}$ is the quasiclassical GF, ω_n is the nth Matsubara frequency, $\vec{n}_{\rm F}$ is the direction of the momentum at the Fermi surface, $v_{\rm F}$ is the magnitude of the Fermi velocity, τ is the collision time, $\check{\tau}_3$ is the third Pauli matrix in Nambu space, μ is the Fermi energy, and $\vec{\eta} = (-\sigma_2, \sigma_1, 0)$, where $\sigma_{1,2}$ are the first and second Pauli matrices in spin space. The tunneling parameter T_1 is nonzero only in FIS regions. To reflect this, we introduce the boundary parameter $\Gamma(x)$:

$$\Gamma(x) = \gamma_0 \Theta\left(|x| - \frac{L_1}{2}\right)\Theta\left(\frac{L}{2} - |x|\right), \tag{3}$$

where Θ denotes the Heaviside function.

The GF is written as $\check{g}\frac{1}{2}(1+\vec{n}_{\rm F}\cdot\vec{\eta})$ to reflect the strong coupling between spin and direction of momentum in a TI. In this paper, a 2D surface of a 3D TI is studied. Therefore, scattering is not prohibited, unlike in a one-dimensional (1D) edge of a 2D TI. In fact, it has been shown experimentally that transport in 3D TIs is not always ballistic [44,45]. We assume the junction is in the dirty limit, that is, the inverse scattering time $\frac{1}{\tau}$ is much larger than any energy scale other than the chemical potential μ. In that case, the GF g is almost isotropic. Thus, it is a good approximation to keep only the zeroth and first term in the expansion in angular momentum, that is,

$$\check{g}\approx\check{g}_s+\vec{n}_{\rm F}\cdot\vec{\check{g}}_a, \tag{4}$$

where the zeroth-order term $\check{g}_s$ and the first-order term $\vec{\check{g}}_a$ satisfy $\check{g}_s^2=\mathbf{1}$ and $\check{g}_s\vec{\check{g}}_a+\vec{\check{g}}_a\check{g}_s=\vec{0}$ to satisfy the normalization condition $\check{g}^2=\check{\mathbf{1}}$ up to second order in τ. The GFs $\check{g}_s$ and $\vec{\check{g}}_a$ do not have any degrees of freedom in momentum space nor in spin space and are thus functions which map position into the space of 2×2 matrices. Using the expansion in angular momentum, the Usadel equation can be derived. The strategy followed to derive the Usadel equation for our structure is very similar to the strategy used in Refs. [41,42]. To this end, we first write

$$\bar{G}_S=\check{G}_{S0}\sigma_0+\vec{\check{G}}_{S1}\cdot\vec{\sigma}, \tag{5}$$

where $\check{G}_{S0}$ and $\vec{\check{G}}_{S1}$ are matrix functions without spin degrees of freedom, and $\vec{\sigma}$ is the vector of Pauli matrices in spin space. It is assumed that the exchange field in the FI always points in the same direction, so that there are no domain walls which may affect the density of states significantly [39]. The position-independent GF in the spin-split SC is

$$\bar{G}_S=\tfrac{1}{2}(1+\vec{b}\cdot\vec{\sigma})\check{G}_\uparrow+\tfrac{1}{2}(1-\vec{b}\cdot\vec{\sigma})\check{G}_\downarrow, \tag{6}$$

$$\check{G}_{\uparrow,\downarrow}=g_{\uparrow,\downarrow}\tau_3+f_{\uparrow,\downarrow}(\cos\phi\tau_1+\sin\phi\tau_2), \tag{7}$$

where $g_{\uparrow,\downarrow}=(\omega_n\pm ih)/\sqrt{(\omega_n\pm ih)^2+\Delta^2}$ are the normal parts, and $f_{\uparrow,\downarrow}=\Delta/\sqrt{(\omega_n\pm ih)^2+\Delta^2}$ are the anomalous parts [46]. The $+$ sign is used for the spin-up component and the $-$ sign for the spin-down component, $\tau_{1,2,3}$ are the Pauli matrices in Nambu space, h is the magnitude of the exchange field $\vec{h}=h\vec{b}$, Δ is the SC potential calculated self-consistently, and ϕ is the phase of the SC. Combining Eq. (5) with Eqs. (6) and (7), we may write

$$\check{G}_{S0,1}=g_{S0,1}\tau_3+f_{S0,1}(\cos\phi\tau_1+\sin\phi\tau_2), \tag{8}$$

$$\vec{\check{G}}_{S1}=\check{G}_{S1}\vec{b}\cdot\vec{\sigma}, \tag{9}$$

where $g_{s0,1}=(g_\uparrow\pm g_\downarrow)/2$ and $f_{S0,1}=(f_\uparrow\pm f_\downarrow)/2$. The component f_{S0} of the condensate is the usual singlet component, whereas f_{S1} is the odd-frequency triplet component [46].

The Usadel equation for the angular-averaged GF g_s without spin degrees of freedom in the TI is obtained analogous to the approach laid out in Ref. [41]. We combine the spin trace of the equation obtained by angular averaging and of the equation obtained by angular averaging after multiplication by $\vec{n}_{\rm F}$. The resulting Usadel equation is

$$D\hat{\nabla}(\check{g}_s\hat{\nabla}\check{g}_s)=\left[\omega_n\check{\tau}_3+\frac{\Gamma(x)}{2}\check{G}_{S0},\check{g}_s\right], \tag{10}$$

with $D=v_{\rm F}^2\tau$. Equation (10) is like the Usadel equation in normal metals. However, the derivative is replaced by a generalized derivative:

$$\hat{\nabla}=\nabla+\frac{\Gamma(x)}{2v_{\rm F}}[\cdot,\check{G}_{S1y}]e_x-\frac{\Gamma(x)}{2v_{\rm F}}[\cdot,\check{G}_{S1x}]e_y. \tag{11}$$

For a spin-split SC, this becomes

$$\hat{\nabla}=\nabla+\frac{\Gamma(x)}{2v_{\rm F}}(b_ye_x-b_xe_y)[\cdot,\check{G}_{S1}]. \tag{12}$$

This derivative is like the derivative presented in Ref. [42] for a TI with an exchange field; in fact, Eq. (10) reduces to this expression if $\check{G}_{S1}=h\check{\tau}_3$. Throughout this paper, we will assume that the magnetic field is oriented perpendicular to the current direction, so that $b_y=1$ and $b_x=0$. The equation is accompanied by the boundary conditions:

$$\hat{\nabla}G_{S1}\left(x=\pm\frac{L}{2}\right)=0. \tag{13}$$

In this paper, we assume that the FI is either very thin or very thick, so that there is no y or z dependence in the problem. As a consequence, the effective one-dimensional equation can be used. From the solutions of Eqs. (10), (12), and (13), one can determine the current:

$$I=\frac{\sigma_{\rm N}}{2}T\sum_n{\rm Tr}[\tau_3\bar{G}(x^*,\omega_n)\hat{\nabla}\bar{G}(x^*,\omega_n)], \tag{14}$$

where $\sigma_{\rm N}$ is the normal state conductance, T is the temperature entering the Matsubara frequencies $\omega_n=(2n+1)\pi T$, and x^* is any position for which $\Gamma(x^*)=0$. The quantities of interest in this paper are the maximum supercurrents I_c^+ and $|I_c^-|$ in both directions and the diode efficiency, defined by

$$\eta=\frac{I_c^+-|I_c^-|}{I_c^++|I_c^-|}. \tag{15}$$

Before showing the numerical solution of the above boundary problem, in the next section, we study the linearized equation in the limit of a small proximity effect. As discussed in the introduction, in this limiting case, the diode effect vanishes, but the anomalous phase ϕ_0 can be studied analytically. The anomalous current is a strong indication for the diode effect to appear.

III. LINEARIZED CASE: THE ϕ_0 JUNCTION

To get an understanding of the physics behind the new Usadel equation, Eq. (10), we focus first on the case of a weak proximity effect and ignore self-consistency of the pair potential. In this case, the anomalous parts of the GF are much smaller than the normal ones, that is, ${\rm Tr}(\tau_{1,2}G)\ll{\rm Tr}(\tau_3G)$, and thus, G can be approximated by

$$G(i\omega_n)\approx\begin{bmatrix}{\rm sgn}(\omega_n) & F\\ \tilde{F} & -{\rm sgn}(\omega_n)\end{bmatrix},$$

where $|F|,|\tilde{F}|\ll1$. Using this approximation, the Usadel equation reduces to a linear equation. We assume here that

the system in Fig. 1(a) is infinite in the x direction. The SC is only absent in the region $(-\frac{L_1}{2}, \frac{L_1}{2})$ and present everywhere outside this region. In this case, Eq. (10) can be written in the three separate spatial regions:

$$\begin{aligned} D\partial_{xx}F &= 2|\omega_n|F - \gamma_0 f_{S0}\exp\left(-i\tfrac{\phi}{2}\right), && x < -\tfrac{L}{2}, \\ D\partial_{xx}F &= 2|\omega_n|F, && |x| < \tfrac{L}{2}, \\ D\partial_{xx}F &= 2|\omega_n|F - \gamma_0 f_{S0}\exp\left(i\tfrac{\phi}{2}\right), && x > \tfrac{L}{2}. \end{aligned} \tag{16}$$

For $x \to \pm\infty$, the GF should commute with $\omega\tau_3 + \check{G}_{S0}$. This implies that the pair potential is given by

$$\lim_{x\to\pm\infty} F = \frac{\gamma_0 f_{S0}}{2|\omega_n|}\exp\left(\pm i\frac{\phi}{2}\right). \tag{17}$$

These are the same equations as for the conventional SC-normal-SC (SNS) junction. However, the equations which join the solutions at $x = \pm\frac{L_1}{2}$ are different from the conventional SNS junction. Requiring continuity of both the GF and the current through the junction yields

$$F\left(\pm\frac{L_1}{2} + 0^+\right) = F\left(\pm\frac{L_1}{2} + 0^-\right), \tag{18}$$

$$\frac{dF}{dx}\left(\pm\frac{L_1}{2} + 0^\pm\right) + \frac{\gamma_0}{v_F} f_{S1}\mathrm{sgn}(\omega_n)\exp\left(\pm i\frac{\phi}{2}\right) = \frac{dF}{dx}\left(\pm\frac{L_1}{2} + 0^\mp\right). \tag{19}$$

This expression differs from the corresponding expression for the SNS junction in the appearance of the f_{S1} term on the left-hand side of Eq. (19). The CPR following from these equations is

$$\begin{aligned} I(\phi) &= \sum_n \frac{1}{4}\exp\left(-2\sqrt{\frac{2|\omega_n|}{D}}\right)\mathrm{Im}\left[(A_n - iB_n)\exp\left(i\frac{\phi}{2}\right)\right]^2 \\ &= \frac{1}{4}\sum_n \exp\left(-2\sqrt{\frac{2|\omega_n|}{D}}\right)\left(A_n^2 - B_n^2\sin\phi + 2A_nB_n\cos\phi\right), \end{aligned} \tag{20}$$

where A_n and B_n are real coefficients given by $A_n = \frac{\gamma_0 f_{S0}}{2|\omega_n|}$ and $B_n = -i\gamma_0 f_{S1}\sqrt{\frac{D\omega_n}{2}}\frac{1}{|\omega_n|}$. This implies that

$$\phi_0 = \arctan 2\frac{\sum_{n=-\infty}^{\infty} A_nB_n\exp\left(-2\sqrt{\frac{2|\omega_n|}{D}}\right)}{\sum_{n=-\infty}^{\infty}\left(A_n^2 - B_n^2\right)\exp\left(-2\sqrt{\frac{2|\omega_n|}{D}}\right)}. \tag{21}$$

The ϕ_0 effect is large if $A_n = B_n$ and small if $|\frac{B_n}{A_n}|$ is not $\sim$1. This ratio is given by

$$\left|\frac{B_n}{A_n}\right| = \frac{\gamma_0|f_{S1}|\sqrt{\frac{D}{2|\omega_n|}}2|\omega_n|}{\gamma_0 f_{S0} v_F} = \frac{|f_{S1}|}{f_{S0}}\frac{1}{v_F}\sqrt{2|\omega_n|D}. \tag{22}$$

Recall that the diffusion constant is given by $D = v_F^2\tau$. This means that $\frac{1}{v_F}\sqrt{2|\omega_n|D} = O(\sqrt{|\omega_n|\tau})$, which is small in the diffusive regime. In fact, in the derivation of the Usadel equation, it is assumed that $\frac{1}{\tau} \gg |\Delta|$, and thus, $\frac{1}{\tau} \gg |\omega_n|$, for every n that contributes significantly to the current. This means the effect can only be large if $f_{S1} \gg f_{S0}$. This constraint can only be satisfied if $h \gg \sqrt{\omega_n^2 + \Delta^2}$ for all Matsubara frequencies that have a significant contribution to the critical current. However, in the setup discussed in this paper, the condition $h \gg \Delta$ cannot be realized since the magnetization is induced via the SC and a high magnetization destroys the superconductivity. Therefore, the ϕ_0 effect is suppressed by a factor $\sqrt{|\omega_n|\tau}$ in the linearized case.

Next, the temperature dependence is discussed. Because the ϕ_0 effect is small, we can simplify the equation for ϕ_0 to

$$\phi_0 \approx 2\frac{\sum_{n=-\infty}^{\infty} A_nB_n\exp\left(-2\sqrt{\frac{2|\omega_n|}{D}}\right)}{\sum_{n=-\infty}^{\infty}\left(A_n^2\right)\exp\left(-2\sqrt{\frac{2|\omega_n|}{D}}\right)}. \tag{23}$$

Now consider the behavior at low temperatures. Since the triplet component f_{S1} is odd in frequency, whereas the singlet component f_{S0} is even in frequency, $|\frac{B_n}{A_n}|$ is small for small Matsubara frequencies. As the temperature is decreased, these terms become more and more dominant in the sum. Thus, at low temperatures, the ϕ_0 effect increases with increasing temperature. On the other hand, for large Matsubara frequencies, the ratio between triplet and singlet components $|\frac{f_{s1}}{f_{s0}}| = O(\frac{h}{|\omega_n|})$. This means that, at high temperatures, the ϕ_0 effect decreases. Therefore, the ϕ_0 effect must be nonmonotonic as a function of temperature; it attains a maximum. Moreover, since $\sqrt{\tau}$ is an ω_n-independent prefactor, it cannot determine the maximum. The temperature at which the maximum is attained is determined by only two dimensionless quantities, $\frac{\Delta}{E_{\mathrm{Th}}}$ and $\frac{h}{\Delta}$.

An interesting limit is the limit in which $\sqrt{\frac{2\pi T}{D}}L_1 \ll 1$ and $h \ll \Delta$ so that the exponential suppression can be ignored to first order in $\sqrt{\frac{2\pi T}{D}}L_1$. The following expression is obtained:[1]

$$\phi_0 \approx \frac{\sum_{n=0}^{\infty} A_nB_n}{\sum_{n=0}^{\infty} A_n^2} = h\sqrt{\tau}\frac{\sum_{n=0}^{\infty}\frac{1}{(\omega_n^2+\Delta^2)^2\sqrt{\omega_n}}}{\sum_{n=0}^{\infty}\frac{1}{\omega_n^4+\Delta^2\omega_n^2}}. \tag{24}$$

The multiplication of the sum with $\sqrt{\tau}$ signals the dirty limit suppression of the ϕ_0 effect. The resulting expression is evaluated numerically as a function of temperature. Numerical evaluation confirmed the nonmonotonicity, see Fig. 2. Because self-consistency of the pair potential is not considered, we only show results for $T/T_c < 0.6$, so that corrections due to self-consistency are small.

In the following sections, we discuss the full nonlinear equation, and we show that the diode effect is nonmonotonic with temperature for short junctions.

IV. NONLINEARIZED CASE: THE SC DIODE EFFECT

To investigate the diode effect, one needs to go beyond the linear approach and numerically solve the Usadel equation. In this section, we present our numerical results for the supercurrent in the FIS-TI-FIS junction. As a first step, it is convenient

[1]Strictly speaking, the linearized case leads to a divergence as T goes to 0. We therefore replace $\Delta/|\omega_n|$ by $\Delta/\sqrt{\omega^2+\gamma_0^2}$, based on the non-linearized case.

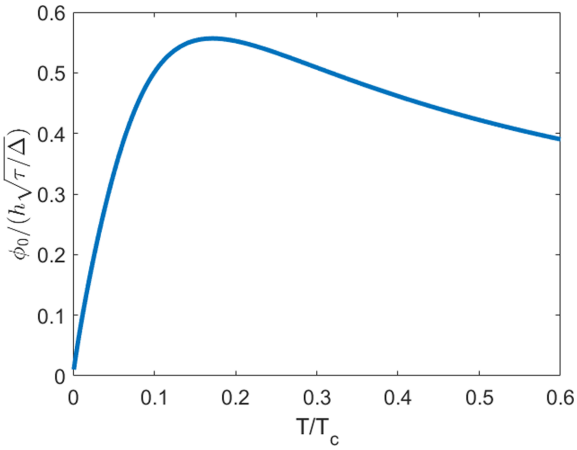

FIG. 2. The ϕ_0 effect as a function of temperature as calculated using Eq. (24). The ϕ_0 effect is suppressed at low temperatures. The ϕ_0 effect is given in units of the small quantity $h\sqrt{\tau/\Delta}$.

to write the Usadel equation, Eq. (10), in dimensionless form, normalizing x by the total length of the junction. The obtained equation is

$$\hat{\nabla}(\check{G}\hat{\nabla}\check{G}) = \left[\frac{\omega_n}{E_{\rm Th}}\check{\tau}_3 + \frac{\Gamma(x)}{2E_{\rm Th}}\check{G}_{S0}, \check{G}\right], \tag{25}$$

$$\hat{\nabla} = \frac{d}{dx} + \frac{\Gamma(x)L}{2v_F}\tilde{b}_y[\check{G}_{S1}, \cdot]. \tag{26}$$

All energies are given in units of the Thouless energy $E_{\rm Th} = \frac{D}{L^2}$, whereas lengths are given in units of L. The strength of the proximity effect is described by the dimensionless parameter $\frac{\gamma_0 L}{v_F} = \frac{\gamma_0}{E_{\rm Th}}\frac{l}{L}$, where $l = v_F\tau$ is the mean free path, which in the diffusive limit must be the shortest length involved in the problem. This puts a constraint on the magnitude of the new dimensionless quantity; it must be much smaller than $\frac{\gamma_0}{E_{\rm Th}}$. However, without this term, the equations reduce to the equations for the SNS junction, which is known not to have a diode effect [14]; it has no time-reversal symmetry breaking. Thus, if the new quantity is very small, the diode effect is very small. Therefore, $\frac{\gamma_0}{E_{\rm Th}}$ must be chosen large, that is, the contact between the SC and the TI must be good to have a large γ_0.

To solve the nonlinearized Usadel equation, Eq. (10), the Riccati parameterization is used:

$$\check{G} = \frac{1}{1+\bar{\gamma}\tilde{\gamma}}\begin{pmatrix} 1-\bar{\gamma}\tilde{\gamma} & 2\gamma \\ 2\tilde{\gamma} & -1+\bar{\gamma}\tilde{\gamma}\end{pmatrix}, \tag{27}$$

where $\bar{\gamma}$ and $\tilde{\gamma}$ are the Riccati parameters.

In principle, the pair potential Δ must be determined self-consistently since it is suppressed by the exchange field [47]. In the numerical calculations, we choose values of the exchange field smaller than $\frac{h}{\Delta_0} = \frac{2}{5}$. Other parameters are set as follows: $\frac{\gamma_0}{E_{\rm Th}} = 25$, whereas $\frac{L_1}{L}$ is chosen to be $\frac{1}{10}$ and $\frac{l}{L} = 0.08 \ll 1$.

Our numerical results for the CPR obtained from the nonlinearized Eq. (10) are shown in Fig. 1(b). There is a finite current value at $\phi = 0$ associated with the appearance of the anomalous phase ϕ_0. Moreover, even though small, there is a difference in the absolute value of the maximum and minimum of the current. This asymmetry reflects the diode effect. By increasing the temperature, both the current at zero phase and the critical current decrease.

We now study the temperature dependence of the diode effect for different exchange fields and sizes of the junction. The numerical results for the diode efficiency are shown in Fig. 3. Interestingly, we find nonmonotonic behavior with a maximum efficiency at a finite temperature T_d. It is important to notice that, by computing η in Fig. 3, the self-consistency of the pair potential is ignored because of the reduction of computational costs. However, we verify that, for all values of h considered, the self-consistency has only a small effect on the magnitude of the gap for temperatures of the order of $T = T_d$. The critical temperatures for all cases shown in Fig. 3(a) are not higher than the temperature indicated using the dashed vertical line.

If the exchange field is increased, Fig. 3(a), the diode efficiency becomes larger. Here, η increases approximately linearly with h. The temperature at which the diode efficiency

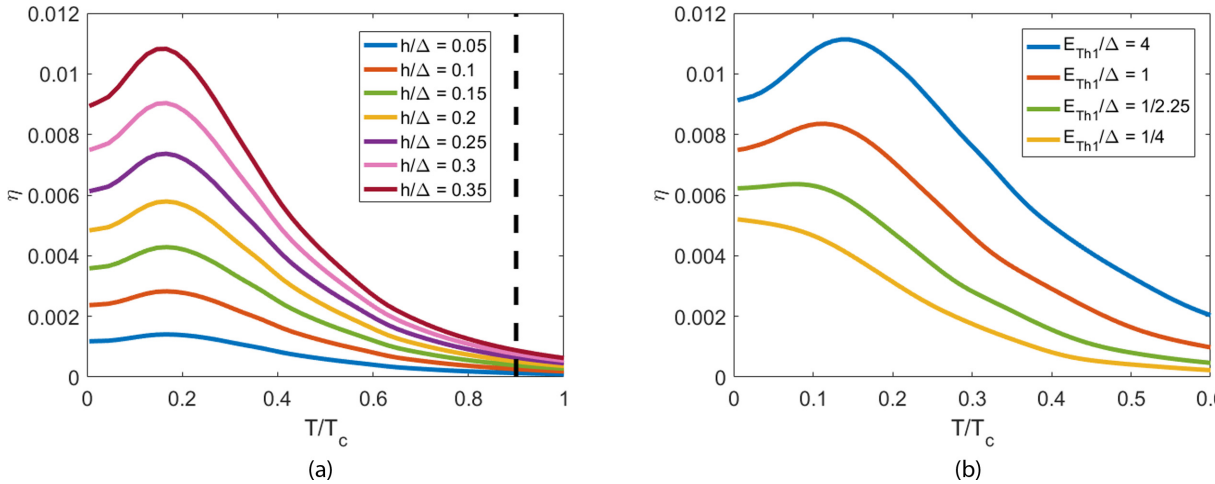

FIG. 3. (a) The temperature dependence of the diode efficiency η for different values of the exchange field strength h, and (b) Thouless energy $E_{\rm Th1} = \frac{D}{L_1^2}$ of the topological insulator (TI) part. The critical temperature is for all magnitudes of the exchange field considered here $>0.9T_c$, highlighted by the black dotted line.

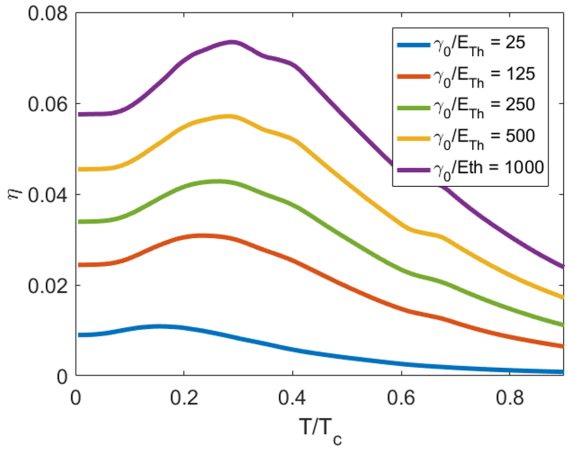

FIG. 4. The diode efficiency as a function of temperature for different values of γ_0.

is maximal is almost independent of the exchange field, with $T_d \approx 0.18$.

We also investigate the influence of the distance between the leads, L_1 on η, see Fig. 3(b). Specifically, $E_{\mathrm{Th1}} = D/L_1^2$ is varied, whereas the quantities $\frac{l}{L}$ and $\frac{L_1}{L}$ are held constant. As the Thouless energy is decreased, the diode efficiency decreases. Moreover, the temperature T_d at which the diode effect is maximal decreases with the length of the junction. For enough long junctions, the dependence of η on temperature becomes monotonic. So far, we have considered disordered systems with low-transparency FIS interfaces. One can, though, increase the ϕ_0 and diode effects by relaxing these conditions. On the one hand, our analytical results in Sec. III indicate that the ϕ_0 effect can be increased by increasing τ; see, for example, Eq. (24). We also verified numerically that the diode effect increases if the degree of disorder decreases.

On the other hand, we also investigated the effect of increasing the ratio $\frac{L_1}{L}$. Our numerical calculations demonstrate that, whereas $I(\phi = 0)/I_c$ increases, the diode effect decreases with increasing $\frac{L_1}{L}$. This can be explained as follows. By increasing the distance L_1 between the electrodes, the CPR becomes more sinuslike. To be precise, we found that, if $\frac{L_1}{L}$ increases from $\frac{1}{10}$ to $\frac{1}{2}$, the ratio between the magnitudes of the second and first harmonics decreases from $\approx\frac{1}{6}$ to $\approx\frac{1}{10}$. As discussed before, in addition to the breaking of time-reversal and inversion symmetries, the diode effect relies crucially on the contribution of higher harmonics to the CPR.

A way to increase the contribution of higher harmonics is to increase the coupling between the SC correlations from the left and right electrodes. This can be achieved by increasing the transparency of the FIS-TI interfaces, as shown in Fig. 4. A restriction is that the parameter γ_0 should be much smaller than $\Delta_0 \frac{\rho_S}{\rho_{\mathrm{TI}}}$, as discussed in the introduction.

Finally, another way to increase the diode effect is by increasing the exchange field, as shown in Fig. 3. In our junction, however, the value of h is limited by the critical field of the SC. To increase the strength of the exchange field without suppressing superconductivity in the S electrodes, one could add additional FI layers directly on top of the TI between the two SCs, like the situation investigated in Ref. [41]. In that case, the exchange field can be larger than the SC gap, and the diode effect may increase.

V. CONCLUSIONS

We present a study of the ϕ_0 and diode effects in a FIS-TI-FIS Josephson junction. Though disorder tends to suppress both effects [26], we found, even in the diffusive limit, sizable effects without applying any external field. We found that, by increasing the FIS-TI interface transparency and the magnetic field, one can increase the diode effect. For short junctions, the diode effect is nonmonotonic as a function of temperature. By increasing the distance between the electrodes, the ϕ_0 effect is enhanced; however, the diode effect is suppressed due to the loss of higher harmonics.

From the point of view of materials, the proposed structure can be fabricated with well-studied material combinations. On the one hand, the use of TIs in Josephson junctions is well understood [44,48–55]. On the other hand, spin-split superconductivity has been measured in several experiments on FIS bilayers, as for example, EuS/Al structures [37,40,56,57]. Moreover, good interfaces between TI and FI have been reported in Ref. [58].

ACKNOWLEDGMENTS

We thank S. Ilić for useful discussions. We acknowledge financial support from the Spanish State Research Agency through Project No. PID2020-114252GB-I00 (SPIRIT). F.S.B. acknowledges financial support from the European Union's Horizon 2020 Research and Innovation Framework Programme under Grant No. 800923 (SUPERTED), the A. v. Humboldt Foundation, and the Basque Government through Grant No. IT-1591-22.

[1] Y. Tanaka, T. Yokoyama, and N. Nagaosa, Manipulation of the Majorana Fermion, Andreev Reflection, and Josephson Current on Topological Insulators, Phys. Rev. Lett. **103**, 107002 (2009).

[2] B. Lu, K. Yada, A. A. Golubov, and Y. Tanaka, Anomalous Josephson effect in *d*-wave superconductor junctions on a topological insulator surface, Phys. Rev. B **92**, 100503(R) (2015).

[3] Y. Tanaka, B. Lu, and N. Nagaosa, Theory of diode effect in *d*-wave superconductor junctions on the surface of topological insulator, arXiv:2205.13177 (2022)

[4] J. J. He, Y. Tanaka, and N. Nagaosa, A phenomenological theory of superconductor diodes, New J. Phys. **24**, 053014 (2022).

[5] R. Wakatsuki, Y. Saito, S. Hoshino, Y. M. Itahashi, T. Ideue, M. Ezawa, Y. Iwasa, and N. Nagaosa, Nonreciprocal charge transport in noncentrosymmetric superconductors, Sci. Adv. **3**, e1602390 (2017).

[6] R. Wakatsuki and N. Nagaosa, Nonreciprocal Current in Noncentrosymmetric Rashba Superconductors, Phys. Rev. Lett. **121**, 026601 (2018).

[7] F. Ando, Y. Miyasaka, T. Li, J. Ishizuka, T. Arakawa, Y. Shiota, T. Moriyama, Y. Yanase, and T. Ono, Observation of superconducting diode effect, Nature (London) **584**, 373 (2020).

[8] B. Pal, A. Chakraborty, P. K. Sivakumar, M. Davydova, A. K. Gopi, A. K. Pandeya, J. A. Krieger, Y. Zhang, M. Date, S. Ju *et al.*, Josephson diode effect from Cooper pair momentum in a topological semimetal, Nature Phys. **18**, 1228 (2022).

[9] C. Baumgartner, L. Fuchs, A. Costa, S. Reinhardt, S. Gronin, G. C. Gardner, T. Lindemann, M. J. Manfra, P. E. Faria Junior, D. Kochan *et al.*, Supercurrent rectification and magnetochiral effects in symmetric Josephson junctions, Nat. Nanotechnol. **17**, 39 (2022).

[10] Y. Hou, F. Nichele, H. Chi, A. Lodesani, Y. Wu, M. F. Ritter, D. Z. Haxell, M. Davydova, S. Ilić, F. S. Bergeret *et al.*, Ubiquitous superconducting diode effect in superconductor thin films, arXiv:2205.09276 (2022).

[11] J.-X. Lin, P. Siriviboon, H. D. Scammell, S. Liu, D. Rhodes, K. Watanabe, T. Taniguchi, J. Hone, M. S. Scheurer, and J. I. A. Li, Zero-field superconducting diode effect in small-twist-angle trilayer graphene, Nat. Phys. **18**, 1221 (2022).

[12] Y.-Y. Lyu, J. Jiang, Y.-L. Wang, Z.-L. Xiao, S. Dong, Q.-H. Chen, M. V. Milošević, H. Wang, R. Divan, J. E. Pearson *et al.*, Superconducting diode effect via conformal-mapped nanoholes, Nat. Commun. **12**, 2703 (2021).

[13] H. Wu, Y. Wang, Y. Xu, P. K. Sivakumar, C. Pasco, U. Filippozzi, S. S. P. Parkin, Y.-J. Zeng, T. McQueen, and M. N. Ali, The field-free Josephson diode in a van der Waals heterostructure, Nature (London) **604**, 653 (2022).

[14] A. A. Golubov, M. Y. Kupriyanov, and E. Il'Ichev, The current-phase relation in Josephson junctions, Rev. Mod. Phys. **76**, 411 (2004).

[15] M. A. Silaev, I. V. Tokatly, and F. S. Bergeret, Anomalous current in diffusive ferromagnetic Josephson junctions, Phys. Rev. B **95**, 184508 (2017).

[16] Y. Zhang, Y. Gu, P. Li, J. Hu, and K. Jiang, General Theory of Josephson Diodes, Phys. Rev. X **12**, 041013 (2022).

[17] M. Z. Hasan and C. L. Kane, Colloquium: Topological insulators, Rev. Mod. Phys. **82**, 3045 (2010).

[18] F. Dolcini, M. Houzet, and J. S. Meyer, Topological Josephson ϕ 0 junctions, Phys. Rev. B **92**, 035428 (2015).

[19] T. Karabassov, I. Bobkova, A. Golubov, and A. Vasenko, Hybrid helical state and superconducting diode effect in S/F/TI heterostructures, arXiv:2203.15608 (2022).

[20] A. A. Reynoso, G. Usaj, C. A. Balseiro, D. Feinberg, and M. Avignon, Anomalous Josephson Current in Junctions with Spin Polarizing Quantum Point Contacts, Phys. Rev. Lett. **101**, 107001 (2008).

[21] A. Buzdin, Direct Coupling Between Magnetism and Superconducting Current in the Josephson φ_0 Junction, Phys. Rev. Lett. **101**, 107005 (2008).

[22] T. Yokoyama, M. Eto, and Y. V. Nazarov, Anomalous Josephson effect induced by spin-orbit interaction and Zeeman effect in semiconductor nanowires, Phys. Rev. B **89**, 195407 (2014).

[23] F. Konschelle, I. V. Tokatly, and F. S. Bergeret, Theory of the spin-galvanic effect and the anomalous phase shift φ_0 in superconductors and Josephson junctions with intrinsic spin-orbit coupling, Phys. Rev. B **92**, 125443 (2015).

[24] F. Bergeret and I. Tokatly, Theory of diffusive φ_0 Josephson junctions in the presence of spin-orbit coupling, EPL **110**, 57005 (2015).

[25] A. Daido, Y. Ikeda, and Y. Yanase, Intrinsic Superconducting Diode Effect, Phys. Rev. Lett. **128**, 037001 (2022).

[26] S. Ilić and F. S. Bergeret, Theory of the Supercurrent Diode Effect in Rashba Superconductors with Arbitrary Disorder, Phys. Rev. Lett. **128**, 177001 (2022).

[27] K.-R. Jeon, J.-K. Kim, J. Yeon, J.-C. Jeon, H. Han, A. Cottet, T. Kontos, and S. S. Parkin, Zero-field polarity-reversible Josephson supercurrent diodes enabled by a proximity-magnetized Pt barrier, Nat. Mater. **21**, 1008 (2022).

[28] R. S. Souto, M. Leijnse, and C. Schrade, The Josephson diode effect in supercurrent interferometers, arXiv:2205.04469 (2022).

[29] X. Hao, J. S. Moodera, and R. Meservey, Thin-Film Superconductor in an Exchange Field, Phys. Rev. Lett. **67**, 1342 (1991).

[30] R. Meservey and P. Tedrow, Spin-polarized electron tunneling, Phys. Rep. **238**, 173 (1994).

[31] T. Tokuyasu, J. A. Sauls, and D. Rainer, Proximity effect of a ferromagnetic insulator in contact with a superconductor, Phys. Rev. B **38**, 8823 (1988).

[32] Y. Tanaka and S. Kashiwaya, Theory of Josephson effect in superconductor-ferromagnetic-insulator-superconductor junction, Phys. C: Supercond. **274**, 357 (1997).

[33] T. T. Heikkilä, M. Silaev, P. Virtanen, and F. S. Bergeret, Thermal, electric and spin transport in superconductor/ferromagnetic-insulator structures, Prog. Surf. Sci. **94**, 100540 (2019).

[34] F. S. Bergeret, M. Silaev, P. Virtanen, and T. T. Heikkilä, Colloquium: Nonequilibrium effects in superconductors with a spin-splitting field, Rev. Mod. Phys. **90**, 041001 (2018).

[35] M. Rouco, S. Chakraborty, F. Aikebaier, V. N. Golovach, E. Strambini, J. S. Moodera, F. Giazotto, T. T. Heikkilä, and F. S. Bergeret, Charge transport through spin-polarized tunnel junction between two spin-split superconductors, Phys. Rev. B **100**, 184501 (2019).

[36] Y. Liu, S. Vaitiekenas, S. Martí-Sánchez, C. Koch, S. Hart, Z. Cui, T. Kanne, S. A. Khan, R. Tanta, S. Upadhyay *et al.*, Semiconductor–ferromagnetic insulator–superconductor nanowires: stray field and exchange field, Nano Lett. **20**, 456 (2020).

[37] E. Strambini, V. N. Golovach, G. De Simoni, J. S. Moodera, F. S. Bergeret, and F. Giazotto, Revealing the magnetic proximity effect in EuS/Al bilayers through superconducting tunneling spectroscopy, Phys. Rev. Mater. **1**, 054402 (2017).

[38] R. Ojajärvi, T. T. Heikkilä, P. Virtanen, and M. A. Silaev, Giant enhancement to spin battery effect in superconductor/ferromagnetic insulator systems, Phys. Rev. B **103**, 224524 (2021).

[39] A. Hijano, V. N. Golovach, and F. S. Bergeret, Quasiparticle density of states and triplet correlations in superconductor/ferromagnetic-insulator structures across a sharp domain wall, Phys. Rev. B **105**, 174507 (2022).

[40] A. Hijano, S. Ilić, M. Rouco, C. González-Orellana, M. Ilyn, C. Rogero, P. Virtanen, T.T. Heikkilä, S. Khorshidian, M. Spies *et al.*, Coexistence of superconductivity and spin-splitting fields in superconductor/ferromagnetic insulator bilayers of arbitrary thickness, Phys. Rev. Res. **3**, 023131 (2021).

[41] A. Zyuzin, M. Alidoust, and D. Loss, Josephson junction through a disordered topological insulator with helical magnetization, Phys. Rev. B **93**, 214502 (2016).

[42] I. V. Bobkova, A. M. Bobkov, A. A. Zyuzin, and M. Alidoust, Magnetoelectrics in disordered topological insulator Josephson junctions, Phys. Rev. B **94**, 134506 (2016).

[43] G. Tkachov, Suppression of surface *p*-wave superconductivity in disordered topological insulators, Phys. Rev. B **87**, 245422 (2013).

[44] M. Veldhorst, M. Snelder, M. Hoek, T. Gang, V. Guduru, X. Wang, U. Zeitler, W. G. van der Wiel, A. Golubov, H. Hilgenkamp *et al.*, Josephson supercurrent through a topological insulator surface state, Nat. Mater. **11**, 417 (2012).

[45] C. Kurter, A. Finck, Y. S. Hor, and D. J. Van Harlingen, Evidence for an anomalous current-phase relation in topological insulator Josephson junctions, Nat. Commun. **6**, 7130 (2015).

[46] F. S. Bergeret, A. F. Volkov, and K. B. Efetov, Odd triplet superconductivity and related phenomena in superconductor-ferromagnet structures, Rev. Mod. Phys. **77**, 1321 (2005).

[47] A. I. Buzdin, Proximity effects in superconductor-ferromagnet heterostructures, Rev. Mod. Phys. **77**, 935 (2005).

[48] M. Veldhorst, M. Snelder, M. Hoek, C. Molenaar, D. P. Leusink, A. A. Golubov, H. Hilgenkamp, and A. Brinkman, Magnetotransport and induced superconductivity in Bi based three-dimensional topological insulators, Phys. Status Solidi RRL **7**, 26 (2013).

[49] M. Snelder, C. Molenaar, Y. Pan, D. Wu, Y. Huang, A. de Visser, A. Golubov, W. van der Wiel, H. Hilgenkamp, M. Golden *et al.*, Josephson supercurrent in a topological insulator without a bulk shunt, Supercond. Sci. Technol. **27**, 104001 (2014).

[50] L. Maier, J. B. Oostinga, D. Knott, C. Brüne, P. Virtanen, G. Tkachov, E. M. Hankiewicz, C. Gould, H. Buhmann, and L. W. Molenkamp, Induced Superconductivity in the Three-Dimensional Topological Insulator HgTe, Phys. Rev. Lett. **109**, 186806 (2012).

[51] I. Sochnikov, L. Maier, C. A. Watson, J. R. Kirtley, C. Gould, G. Tkachov, E. M. Hankiewicz, C. Brüne, H. Buhmann, L. W. Molenkamp *et al.*, Nonsinusoidal Current-Phase Relationship in Josephson Junctions from the 3D Topological Insulator HgTe, Phys. Rev. Lett. **114**, 066801 (2015).

[52] J. Wiedenmann, E. Bocquillon, R. S. Deacon, S. Hartinger, O. Herrmann, T. M. Klapwijk, L. Maier, C. Ames, C. Brüne, C. Gould *et al.*, 4π-periodic Josephson supercurrent in HgTe-based topological Josephson junctions, Nat. Commun. **7**, 10303 (2016).

[53] J. B. Oostinga, L. Maier, P. Schüffelgen, D. Knott, C. Ames, C. Brüne, G. Tkachov, H. Buhmann, and L. W. Molenkamp, Josephson Supercurrent through the Topological Surface States of Strained Bulk HgTe, Phys. Rev. X **3**, 021007 (2013).

[54] A.-Q. Wang, C.-Z. Li, C. Li, Z.-M. Liao, A. Brinkman, and D.-P. Yu, 4π-Periodic Supercurrent from Surface States in Cd_3As_2 Nanowire-Based Josephson Junctions, Phys. Rev. Lett. **121**, 237701 (2018).

[55] P. Mandal, N. Taufertshöfer, L. Lunczer, M. P. Stehno, C. Gould, and L. Molenkamp, Finite field transport response of a dilute magnetic topological insulator-based Josephson junction, Nano Lett. **22**, 3557 (2022).

[56] J. S. Moodera, X. Hao, G. A. Gibson, and R. Meservey, Electron-Spin Polarization in Tunnel Junctions in Zero Applied Field with Ferromagnetic EuS Barriers, Phys. Rev. Lett. **61**, 637 (1988).

[57] Y. M. Xiong, S. Stadler, P. W. Adams, and G. Catelani, Spin-Resolved Tunneling Studies of the Exchange Field in EuS/Al Bilayers, Phys. Rev. Lett. **106**, 247001 (2011).

[58] P. Wei, F. Katmis, B. A. Assaf, H. Steinberg, P. Jarillo-Herrero, D. Heiman, and J. S. Moodera, Exchange-Coupling-Induced Symmetry Breaking in Topological Insulators, Phys. Rev. Lett. **110**, 186807 (2013).

Correction: Four references and their citations in text were missing and have been inserted in the first sentence of the paper.